Macromolecules

ARTICLE

pubs.acs.org/Macromolecules

Homogeneous Dynamics within Inhomogeneous Environment in Semicrystalline Polymers

Alejandro Sanz,[†] Aurora Nogales,[†] Tiberio A. Ezquerra,*[,†] Wolfgang Häussler,[‡] Michelina Soccio,[§] Nadia Lotti,[§] and Andrea Munari[§]

[†]Instituto de Estructura de la Materia, CSIC, Serrano 121, 28006 Madrid, Spain

[‡]Forschungs-Neutronenquelle Heinz Maier-Leibnitz (FRM II), Garching, Germany

[§]Dipartimento di Ingegneria Civile, Ambientale e dei Materiali-Universitá di Bologna, Via Terracini 28, 40131 Bologna, Italy

ABSTRACT:

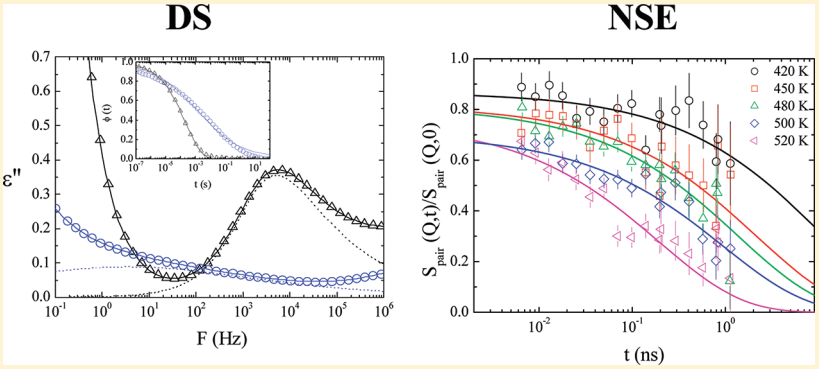

We show that the combination of dielectric with neutron spin echo measurements performed in a model deuterated polymer as poly(ethylene terephthalate) suggests that the dynamics of semicrystalline polymers occurs in an homogeneous scenario similar to that valid to describe the dynamics of amorphous polymers. Accordingly, the intermolecular cooperativity is expected to be rather similar in both amorphous and semicrystalline polymers. The reduced segmental mobility of the semicrystalline polymer is restricted to well differentiate regions, probably in the crystal−amorphous interface. The significant broadening of the dielectric segmental relaxation in semicrystalline polymers can be attributed to the averaging effect of measuring a homogeneous relaxation with similar stretching exponents over an inhomogeneous environment.

1. INTRODUCTION

Semicrystalline polymers are present in our everyday life in such a way that about two-thirds of the annual production of synthetic polymers mainly consists on this type of material. Semicrystalline polymers usually can develop a characteristic folded chain crystalline lamellar morphology[1,2] of nanometer dimensions when located in the temperature range of supercooling defined by the glass transition temperature, T_g, and the equilibrium melting temperature, T^0_m. The lamellar morphology consists of stacks of laminar crystals with amorphous regions intercalated between them. While the crystalline phase provides strength, the amorphous one provides toughness to the material. The amorphous phase in a semicrystalline polymer can be considered as self-confined within the restricted environment imposed by the crystalline phase. A strong interaction between the amorphous phase and the crystalline one is expected as polymer chains in the former are physically connected with the crystals. This particular case of confinement in which both confining and confined phase are the same material shifts T_g toward higher values.[3] The segmental dynamics, giving rise to the α-relaxation, is also significantly affected.[4] Above T_g, the confinement effects are reflected in the dielectric α-relaxation by a decrease of its dielectric strength, an increase of the relaxation time, and a broadening of the relaxation process.[3−7] These effects resemble very much those observed in ultrathin polymer films deposited over highly interacting substrates,[8] polymers confined within nanopores,[9] or nanochannels with attracting surfaces.[10] A general feature of supercooled liquids in general and of amorphous polymers in particular is that they approach equilibrium in a nonexponential way in response to an external perturbation. This behavior can be visualized by invoking two different scenarios.[11,12] In the first one, it is assumed the existence of a heterogeneous set of environments in which relaxation takes place exponentially but the relaxation time varies among environments. In a second one, every molecule or polymer segment relaxes intrinsically in a nonexponential manner within a homogeneous environment. Different kind of experiments have shown that for both glass-forming liquids[11] and amorphous polymers[13] the homogeneous scenario seems to be valid. The stretched exponential or Kohlrausch−Williams−Watts (KWW) equation is currently used

Received: June 14, 2011
Revised: September 8, 2011
Published: September 28, 2011

to characterize the response function[14,15]

$$\varphi(t) \propto \exp\left[-\left(\frac{t}{\tau_{KWW}}\right)^{\beta}\right] \quad (1)$$

where τ_{KWW} is the characteristic relaxation time. As far as the α-relaxation is concerned, the stretching exponent, β, has been experimentally related to the degree of intermolecular coupling,[16] showing higher coupling those systems with lower β value. Values of $\beta \approx 0.5$ are typical for amorphous polymers.[17] In contrast, much broader segmental dynamics is observed for semicrystalline polymers[3,5,18,19] which may render values as low as $\beta \approx 0.2$. This effect was proposed to be due to an inhomogeneous broadening caused by the constraint of the segments in the proximity of the crystals.[16,20] However, until now a direct evidence of this assumption has not been provided. The temperature dependence of the segmental relaxation time in supercooled polymers departs from the Arrhenius equation. On the basis of this observation, supercooled liquids can be classified as *Strong* or *Fragile* depending on the degree of departure from an Arrhenius behavior of their α-relaxation time temperature dependencies.[12] Polymers are typically fragile liquids[21] with a temperature dependence of the segmental relaxation time described by the Vogel–Tammann–Fulcher (VFT) equation

$$\tau(T) \propto \exp\left[\frac{DT_0}{T - T_0}\right] \quad (2)$$

where D is referred to as the fragility strength parameter. The fragility index m, currently use to characterize the dynamical fragility, can be defined as

$$m = \left[\frac{\partial \log \tau}{\partial(T_g/T)}\right]_{T=T_g} = 16 + \frac{590}{D} \quad (3)$$

Fragility is usually correlated to the stretching exponent, β, for many materials.[21] From the point of view of the potential energy landscape (PEL) perspective, fragile systems display a proliferation of well-separated basins which result in a broad spectrum of relaxation times leading to stretched exponential dynamics.[22,23] The correlation is also consistent within the framework of the coupling model (CM).[16] For glass-forming liquids this correlation has been empirically described[21] by the following relation

$$m = m_0 - s\beta \quad (4)$$

with $m_0 = 250 \pm 30$ and $s = 320$. This relation suggests that the more fragile the system is the more nonexponential the relaxation functions will be. In spite of the significant broadening of the segmental relaxation in semicrystalline polymers in comparison with that of amorphous ones, neither the degree of intermolecular coupling nor the fragility, as derived from the fragility plots ($\log[\tau]$ vs T_g/T), seems to be severely affected by the presence of the crystalline phase.[16,24] An absence of significant effect on fragility has also been reported to occur in ultrathin polymer films deposited over highly interacting substrates.[8] Whether this apparent mismatch between broadening of the relaxation and dynamical fragility is caused by inhomogeneous broadening due to the intrinsic structural heterogeneity of a semicrystalline polymer or to a modification of the dynamical scenario provoked by the confinement of the amorphous phase by the crystalline one is a question that can be solved by neutron spin echo. This technique offers a direct molecular assessment of dynamical processes both in space and in time.[17]

In this paper, by combining dielectric spectroscopy (DS) with neutron spin echo spectroscopy (NSE), we report on a direct observation of the intermediate scattering function, or the dynamic structure factor, on a fully deuterated sample of poly(ethylene terephthalate). By doing NSE measurements above the T_g of the polymer in the Q-range close to the first static structure factor maximum, we were able to have access to the dynamics governed by the α-relaxation. Since the functional form of the dynamic structure factor is formally a KWW function, we could asses directly the broadening of the α-relaxation by measuring the stretching exponent β. Our results suggest that the segmental dynamics in semicrystalline polymers has a homogeneous nature being intrinsically nonexponential. That means that the degree of intermolecular coupling is very similar for amorphous and semicrystalline polymers. However, the structural inhomogeneity causes an inhomogeneous broadening of the α-relaxation which mainly affects intramolecular coupling.

2. EXPERIMENTAL PART

Deuterated poly(ethylene terephthalate) (d-PET) was synthesized in bulk starting from deuterated terephthalic acid and deuterated ethylene glycol in a molar ratio 1:2, employing $Ti(OBu)_4$ as catalyst. The polymer was obtained with a molecular weight of M_n = 15 000 g/mol and a M_w = 29 000 g/mol. The polymer chemical structure was determined by means of ^{13}C NMR spectroscopy, and molecular weight data were obtained by gel permeation chromatography. The calorimetric glass transition temperature of the amorphous and semicrystalline specimens was 341 and 345 K, respectively. The melting temperature of the semicrystalline sample, as derived by calorimetry, was T_m = 527 K. The semicrystalline specimen was obtained by slow cooling from the molten state with a crystalliny of $X_c = 32.5 \pm 2.5\%$ as estimated by wide-angle X-ray scattering and calorimetry measurements. Small-angle X-ray scattering of the semicrystalline specimen provides an estimate of the length of the amorphous region among crystals of about 3 nm. Dielectric loss measurements, $\varepsilon'' = \mathrm{Im}(\varepsilon^*)$, were performed over a broad frequency window, $10^{-1} \le F\ (\mathrm{Hz}) \le 10^7$, by means of a Novocontrol system integrating a dielectric interface (ALPHA) and a temperature control by nitrogen jet (QUATRO) with a temperature error, during every single sweep in frequency, of ±0.1 K. Neutron spin echo (NSE) experiments were performed at the RESEDA instrument at the FRM II Munich, Germany, at a Q value for the scattering vector of 13.8 nm^{-1} and at different temperatures in the Fourier intervals 0.001 ns $\le t \le$ 5 ns, restricted to 2 ns as maximum, with an incident wavelength of λ = 0.545 nm.

3. RESULTS AND DISCUSSION

Figure 1 shows ε'' data at T = 363 K as a function of frequency $F = \omega/(2\pi)$, being ω the angular frequency, for the amorphous and semicrystalline deuterated PET specimens. Similarly as for standard hydrogenated PET, the α-relaxation for the amorphous deuterated PET appears as a maximum in ε'' that can be described by means of the Havriliak–Negami (HN) function:[5,6,25]

$$\varepsilon'' = \mathrm{Im}[\varepsilon^*(\omega)] = \mathrm{Im}\left[\varepsilon_\infty + \sum_{x=\alpha,\beta}\left(\frac{\Delta\varepsilon_x}{[1 + (i\omega\tau^x_{HN})^{b_x}]^{c_x}}\right)\right] \quad (5)$$

where the subscript indicates either the α or the β relaxation, $\Delta\varepsilon_x$ is the relaxation strength, τ^x_{HN} is the most probable relaxation time

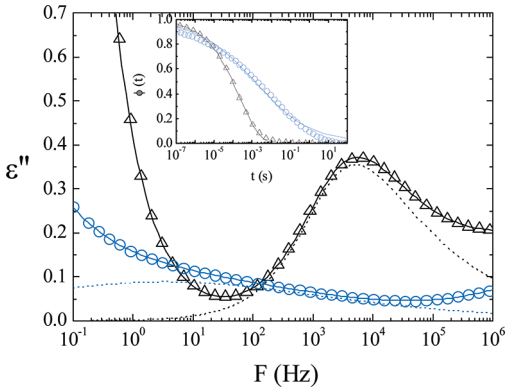

Figure 1. Dielectric loss values, ε'', as a function of frequency at $T = 363$ K for the amorphous (△) and semicrystalline (○) d-PET sample. Continuous and dotted lines represent the fits to the HN equation of the total relaxation spectra and of the individual α-relaxations, respectively. The inset shows the corresponding numerically calculated dipole moment time correlation functions. The continuous lines indicate the best fittings of the calculated data to the KWW equation.

of the relaxation time distribution function, and b_x, c_x are the shape parameters which describe respectively the symmetric and asymmetric broadening of the relaxation time distribution function. An additional term of the form $(\sigma_0/(\varepsilon_{vac}\omega))^s$ has to be added in order to account for the contribution of the dc conductivity, σ_0, at lower frequencies being ε_{vac} the real permittivity of vacuum. The exponent s depends on the conduction mechanism.[25] The procedure to separate the different contributions of the dielectric spectrum of PET has been extensively described in the literature.[3−6] Therefore, in Figure 1 only the global fit of the HN function to the experimental data (continuous line) and the contribution of the α-relaxation (dotted line) are shown for the sake of clarity.

The α-relaxation for the amorphous specimen appears as an asymmetric process characterized by shape parameters $b = 0.76$ and $c = 0.43$. On the contrary the α-relaxation for the semicrystalline specimen appears as a much broader process, $b = 0.23$, and essentially symmetric, $c = 1$. As mentioned in the Introduction, this difference is rather universal upon comparing the segmental relaxation of amorphous and semicrystalline polymers.[5−7] The dielectric loss ε'' is related to the dipole moment time correlation function, $\phi(t)$, by a pure imaginary Laplace transformation.[26] Inversely, it can be shown that

$$\phi(t) = \frac{2}{\pi}\int_0^\infty \left(\frac{\varepsilon''(\omega)}{\Delta\varepsilon}\right)\cos(\omega t)\frac{d\omega}{\omega} \qquad (6)$$

This equation can be numerically solved considering the HN shape parameters characterizing the α-process in the frequency domain.[27−29] The inset of Figure 1 shows the dipole moment time correlation functions, $\phi(t)$, calculated by means of the software WinFIT[29] for the α-relaxation of the amorphous and semicrystalline specimens. The continuous lines indicate the best fittings of the KWW equation to the experimental data. A stretching exponent value of $\beta \approx 0.4$ is obtained for the amorphous sample while a significant lower value of $\beta \approx 0.2$ for the semicrystalline one. As mentioned before, this is a characteristic upon comparing the α-relaxation of semicrystalline and amorphous polymers. Figure 2 represents in a fragility plot the values of τ_{KWW} and those of the stretching exponents, β, obtained from the fitting of eq 1 to the dielectric data for the amorphous and semicrystalline d-PET samples. Graphically, the slopes as $T_g/T \rightarrow 1$ exhibit small

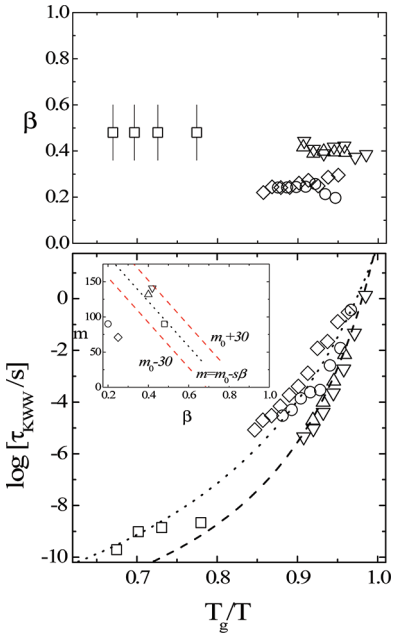

Figure 2. Fragility plot for the values of β (top) and of τ_{KWW} (bottom) obtained from the fitting of eq 1 to the dielectric data for the amorphous (△) and semicrystalline (○) d-PET samples and for the amorphous (▽) and semicrystalline (◇) hydrogenated ones. NSE data for semicrystalline (□) d-PET. The inset shows a graphical representation of m (eq 4) with boundaries[21] in m_0 including values of fragility and stretching exponents.

differences between the amorphous and semicrystalline d-PET. However, estimates of the fragility parameters according to eq 3 give values of $m = 90$ and $m = 141$ for semicrystalline and amorphous specimens, respectively. The β values are nearly temperature independent remaining in a value close to ≈0.4 and ≈0.2 for the amorphous and semicrystalline samples, respectively. Interestingly enough, the difference in fragility of the amorphous component in the semicrystalline polymer as compared to that of the purely amorphous one is in agreement with recent computational and experimental work, indicating that the grain boundary region of polycrystalline materials generally has the character of a glass-forming liquid, even in the diverse situations of metallic materials such as Ni, polycrystalline granular, and colloidal materials,[30] where the degree of fragility of the amorphous boundary fluid depends on the grain boundary geometry. For the sake of comparison, data for amorphous and semicrystalline hydrogenated PET have been included in Figure 2. As one sees both deuterated and hydrogenated samples behave in a similar manner. The inset of Figure 2 graphically represents the empirical relation among m and β with the estimated boundaries depending on m_0. By including fragility and stretching exponent values corresponding to amorphous PET, it is evidenced that for both deuterated and hydrogenated samples the relation provided by eq 4 is fulfilled. However, by including the corresponding values for the semicrystalline samples, one sees that they lay well far away from the boundaries defined by eq 4, indicating a breakage of the relation between dynamical fragility and segmental stretching exponents.

Further information which can help to understand this apparent discrepancy can be gained by the neutron spin echo (NSE) measurements which were accomplished in semicrystalline d-PET.

dx.doi.org/10.1021/ma201304p |*Macromolecules* 2011, 44, 8124–8128

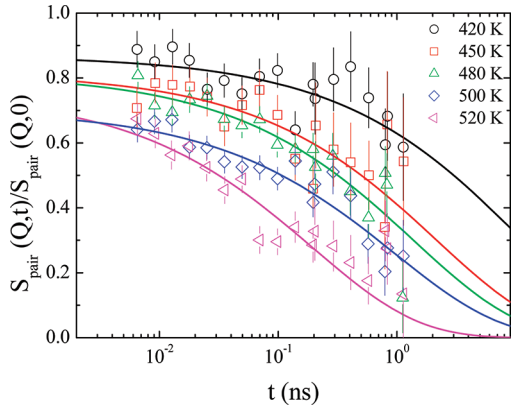

Figure 3. Time evolution of the dynamic structure factor of semicrystalline deuterated PET at $Q = 13.8\ nm^{-1}$ at different temperatures above T_g. Continuous lines correspond to the fits of the KWW function to the experimental data.

Figure 3 shows the dynamic structure factor obtained from the NSE experiments on semicrystalline d-PET at $Q = 13.8\ nm^{-1}$ and at different temperatures above T_g.

This Q value was carefully chosen in order to be as close as possible to the maximum of the static structure factor peak of amorphous PET ($Q_{max} = 14.9\ nm^{-1}$) and also to avoid any of the Bragg peaks appearing from the unavoidable crystalline diffraction of the semicrystalline specimen.[6] At first glance it is seen that the experimental data of normalized $S_{pair}(Q,t)$ exhibit a stretched time evolution with characteristic decay times becoming faster the higher the temperature. As previously discussed, the dynamics of the density fluctuations in the proximity of the structure factor maximum is governed by the α-relaxation.[17,31] Considering that the functional form for this process is the KWW function, then for the NSE dynamic structure factor the following time dependence can be written:[17,31]

$$\frac{S_{pair}(Q,t)}{S_{pair}(Q,0)} \propto \exp\left[-\left(\frac{t}{\tau_{NSE}(Q)}\right)^{\beta}\right] \qquad (7)$$

where $\tau_{NSE}(Q)$ represents the Q-dependent characteristic time of the relaxation as measured by NSE. Accordingly, NSE experiments allows one to estimate independently both $\tau_{NSE}(Q)$ and β. The results for $\tau_{NSE}(Q)$ and β have been included in Figure 2 for comparison with the dielectric ones. Only temperatures $T > 420$ K has been considered in order to allow NSE data to accommodate well into the dynamic range of the spectrometer. The values of $\tau_{NSE}(Q)$ fit reasonably well into the VFT function corresponding to the dielectric data obtained for the deuterated semicrystalline polymer, indicating that both techniques are exploring the α-relaxation under the present conditions. However, a significant discrepancy is observed for the β stretching exponent upon comparing NSE and dielectric data for the semicrystalline d-PET. The data analysis presented here reveals that while the dielectric response of the semicrystalline polymer associated with the α-relaxation would require a very broad KWW function with $\beta \approx 0.2$ the corresponding decay function measured by NSE provided a value of $\beta \approx 0.5$. Curiously enough, the values of β_{NSE} for the semicrystalline sample are closer to the dielectric ones of the amorphous polymer. Moreover, if we consider the obtained values of β from NSE and we replot the data for the semicrystalline deuterated polymer in the inset of Figure 2, then the value returns to be within the limits of what it is expected by eq 4. All these results point toward the existence of a homogeneous dynamics in the case of a semicrystalline polymer since the value of β_{NSE} is close to that observed for the amorphous polymer and both are within the expectations for homogeneous dynamics in amorphous polymers.[17] Consequently, we can propose that the dynamic scenario for the α-relaxation of a semicrystalline polymer is that of the homogeneous case. In other words, there is no change of dynamic scenario induced by the crystalline phase confinement. Previous NSE experiments performed in self-assembled alkyl nanodomains in high-order poly(*n*-alkyl methacrylates) have shown[32] that side chains anchored to the main chain exhibit a strong gradient of mobilities rendering a dynamic structure factor which decays logarithmically instead of being a KWW function. This observation would indicate, in our case, that the reduced segmental mobility of the semicrystalline polymer is restricted to well-differentiated regions of the sample, probably in the crystal−amorphous interface, since the dynamic structure factor is well described by the KWW function. However, it is clear that the segmental relaxation time becomes slower for a semicrystalline polymer as compared with that of the amorphous one (Figure 1). It is worth mentioning that the behavior described here is different from that observed for poly(vinyl chloride) (PVC) where a continuous increment with temperature of the β exponent has been observed[31] for $T > T_g$. PVC exhibits peculiar structural heterogeneities characterized by the presence of a well-defined correlation maxima observed in small-angle scattering measurements and an absence of Bragg maxima[31] at wider scattering angles. In this respect PVC cannot be strictly considered as a canonical semicrystalline polymer. The main difference between PVC and PET is that the structural heterogeneities of the former may continuously change with temperature[31] for $T > T_g$. This effect is likely to produce a temperature changing structural environment for the α-relaxation. However for PET, the true semicrystalline nature of the polymer, characterized by the presence of Bragg maxima[6] at wide scattering angles, is not modified until temperatures close to T_m are reached. Within the frame of the coupling model, the time dependence of the segmental relaxation time is given by[18] $\tau = [\tau_0 t_c^{\beta-1}]^{1/\beta}$, where τ_0 is an intermolecularly uncorrelated (intramolecular) relaxation time[33] and t_c is a crossover time at which the segmental relaxation assumes a KWW form. Accordingly, even assuming that intermolecular cooperativity does not change upon comparing the dynamics of amorphous and semicrystalline polymers, a slowdown of the dynamics can be expected if a concurrent slowing down of the intramolecular mobility occurs. Since in semicrystalline polymers chains in the amorphous phase are tightly bounded to the crystalline one, a significant intramolecular restriction in mobility is very likely to appear. While NSE measurements are performed at particular Q values and therefore explore a given length scale of the order of $2\pi/Q$, dielectric measurements can be considered as taken at $Q \approx 0$ implicitly involving a certain average over a broad range of length scales and also a broader dynamic range than that covered by NSE. Accordingly, dielectric measurements of the α-relaxation in a semicrystalline polymer can be considered to provide an average relaxation curve averaged over the different environments. Because of the intrinsic structural inhomogeneity of a semicrystalline polymer, the environment is also inhomogeneous, and therefore the dielectric segmental relaxation appears as an extremely broad process.

In summary, the combination of dielectric and neutron spin echo measurements performed in a model deuterated polymer,

poly(ethylene terephthalate), have shown that the dynamics of semicrystalline polymers occurs in an homogeneous scenario similar to that valid to describe the dynamics of amorphous polymers. This is so because β_{NSE} for the semicrystalline polymer is very close to β_{DS} of the amorphous one. Accordingly, the intermolecular cooperativity is expected to be rather similar in both amorphous and semicrystalline polymers. The slowing down of the characteristic segmental relaxation in a semicrystalline polymer in comparison with that of an amorphous one seems to be caused by a retardation of the intramolecular mobility provoked by the anchoring of the polymers chains of the amorphous phase bounded to the crystalline one. The reduced segmental mobility of the semicrystalline polymer is restricted to well differentiate spatial regions, probably in the crystal–amorphous interface. The significant broadening of the dielectric segmental relaxation in semicrystalline polymers can be attributed to the averaging effect of measuring a homogeneous relaxation with similar β values over an inhomogeneous environment providing different characteristic relaxation times.

■ ACKNOWLEDGMENT

We are indebted to MICINN (Spain) for financial support through Grants MAT2009-07789 and MAT2008-03232. A.S. thanks the Spanish Research Council (CSIC) for a JAE-doc tenure.

■ REFERENCES

(1) Bassett, D. C. *Principles of Polymer Morphology*; Cambridge University Press: Cambridge, 1981.
(2) Welch, P.; Muthukumar, M. *Phys. Rev. Lett.* **2001**, *87*, 21.
(3) Coburn, J. C.; Boyd, R. H. *Macromolecules* **1986**, *19* (8), 2238–2245.
(4) Nogales, A.; Ezquerra, T. A.; Denchev, Z.; Sics, I.; Calleja, F. J. B.; Hsiao, B. S. *J. Chem. Phys.* **2001**, *115* (8), 3804–3813.
(5) Fukao, K.; Miyamoto, Y. *Phys. Rev. Lett.* **1997**, *79* (23), 4613–4616.
(6) Alvarez, C.; Sics, I.; Nogales, A.; Denchev, Z.; Funari, S. S.; Ezquerra, T. A. *Polymer* **2004**, *45* (11), 3953–3959.
(7) Soccio, M.; Nogales, A.; Lotti, N.; Munari, A.; Ezquerra, T. A. *Phys. Rev. Lett.* **2007**, *98* (3), xxxx.
(8) Napolitano, S.; Prevosto, D.; Lucchesi, M.; Pingue, P.; D'Acunto, M.; Rolla, P. *Langmuir* **2007**, *23* (4), 2103–2109.
(9) Schuller, J.; Richert, R.; Fischer, E. W. *Phys. Rev. B* **1995**, *52* (21), 15232–15238.
(10) Martin, J.; Mijangos, C.; Sanz, A.; Ezquerra, T. A.; Nogales, A. *Macromolecules* **2009**, *42* (14), 5395–5401.
(11) Richert, R. *J. Non-Cryst. Solids* **1994**, *172*, 209–213.
(12) Ediger, M. D.; Angell, C. A.; Nagel, S. R. *J. Phys. Chem.* **1996**, *100* (31), 13200–13212.
(13) Arbe, A.; Colmenero, J.; Monkenbusch, M.; Richter, D. *Phys. Rev. Lett.* **1998**, *81* (3), 590–593.
(14) Williams, G.; Watts, D. C. *Trans. Faraday Soc.* **1970**, *66* (565P), 80.
(15) Cardona, M.; Chamberlin, R. V.; Marx, W. *Ann. Phys.* **2007**, *16* (12), 842–845.
(16) Ngai, K. L.; Roland, C. M. *Macromolecules* **1993**, *26* (11), 2688–2690.
(17) Richter, D.; Monkenbusch, M.; Arbe, A.; Colmenero, J. *Neutron Spin Echo in Polymer Systems*; Springer: Berlin, 2005.
(18) Ngai, K. L.; Roland, C. M. *Macromolecules* **1993**, *26* (25), 6824–6830.
(19) Ezquerra, T. A.; Majszczyk, J.; Baltacalleja, F. J.; Lopezcabarcos, E.; Gardner, K. H.; Hsiao, B. S. *Phys. Scr.* **1994**, *55*, 212–215.
(20) Roland, C. M. *Macromolecules* **1994**, *27* (15), 4242–4247.
(21) Bohmer, R.; Ngai, K. L.; Angell, C. A.; Plazek, D. J. *J. Chem. Phys.* **1993**, *99* (5), 4201–4209.
(22) Debenedetti, P. G.; Stillinger, F. H. *Nature* **2001**, *410* (6825), 259–267.
(23) Abraham, S. E.; Bhattacharrya, S. M.; Bagchi, B. *Phys. Rev. Lett.* **2008**, *100*, 16.
(24) Nogales, A.; Ezquerra, T. A.; Batallan, F.; Frick, B.; Lopez-Cabarcos, E.; Balta-Calleja, F. J. *Macromolecules* **1999**, *32* (7), 2301–2308.
(25) Kremer, F., Schönhals, A., Eds. *Broadband Dielectric Spectroscopy*; Springer: Berlin, 2002.
(26) Cook, M.; Watts, D. C.; Williams, G. *Trans. Faraday Soc.* **1970**, *66* (574), 2503.
(27) Boese, D.; Momper, B.; Meier, G.; Kremer, F.; Hagenah, J. U.; Fischer, E. W. *Macromolecules* **1989**, *22* (12), 4416–4421.
(28) Hagenah, J.-U.; Meier, G.; Fytas, G.; Fischer, E. W. *Polym. J.* **1987**, *19*, 441.
(29) WinFIT Curve Fitting Software, Novocontrol Technologies GmbH.
(30) Zhang, H.; Srolovitz, D. J.; Douglas, J. F.; Warren, J. A. *Proc. Natl. Acad. Sci. U. S. A.* **2009**, *106* (19), 7735–7740.
(31) Arbe, A.; Moral, A.; Alegria, A.; Colmenero, J.; Pyckhout-Hintzen, W.; Richter, D.; Farago, B.; Frick, B. *J. Chem. Phys.* **2002**, *117* (3), 1336–1350.
(32) Arbe, A.; Genix, A. C.; Colmenero, J.; Richter, D.; Fouquet, P. *Soft Matter* **2008**, *4* (9), 1792–1795.
(33) Helfand, E. *Science* **1984**, *226* (4675), 647–650.